Polymer 50 (2009) 3739–3746

Contents lists available at ScienceDirect

Polymer

journal homepage: www.elsevier.com/locate/polymer

Characterization of latex-based isotactic polypropylene/clay nanocomposites

Luljeta Raka [a,*], Gordana Bogoeva-Gaceva [b], Kangbo Lu [c,d], Joachim Loos [c,d]

[a] Faculty of Natural Sciences and Mathematics, State University of Tetovo, Blvd Ilinden, 1200 Tetovo, Macedonia
[b] Faculty of Technology and Metallurgy, University St. Cyril and Methodious, 16 Rudjer Boskovic, 1000 Skopje, Macedonia
[c] Laboratory of Materials and Interface Chemistry, Eindhoven University of Technology, 5600 MB, The Netherlands
[d] Dutch Polymer Institute, P.O. Box 902, 5600 AX Eindhoven, The Netherlands

ARTICLE INFO

Article history:
Received 28 January 2009
Accepted 21 May 2009
Available online 29 May 2009

Keywords:
Nanocomposite
Polypropylene
Organo-modified clay

ABSTRACT

Polypropylene/clay nanocomposite (PCN) containing 1 wt% organo-modified clay was prepared by latex technology, previously successfully applied for preparation of carbon nanotubes (CNTs)/polymer composites. The level of dispersion of organoclay and the microstructure of the resulting PCNs were characterized by means of X-ray diffraction analysis, transmission electron microscopy (TEM), and scanning electron microscopy (SEM). The obtained results have demonstrated that the latex technique represents a promising method for preparation of PP/clay nanocomposites with good dispersion of exfoliated nanoclay particles. The influence of clay nanoparticles on nonisothermal crystallization of PCN was investigated by DSC. The crystallization onset temperature of the matrix rises for about 5 °C when crystallizing from the quiescent melt. Improved thermal stability of PP/nanoclay was observed as evaluated by TGA. The dynamic mechanical analysis reveals an increase in storage modulus of PP matrix in the nanocomposites for 30% over a temperature range, indicating an increase in the stiffness of the material with the addition of organically modified clay.

1. Introduction

Polymer/clay nanocomposites have great potential as low-cost, lightweight and high-performance materials because of the physical property enhancements due to their improved mechanical, thermal, electrical and optical properties as compared to their macro- and micro-counterparts [1]. It has been shown that polymer/clay nanocomposites have not only reduced flammability, but also improved mechanical properties that is not a case with many flame retardants, which also reduce the mechanical properties of the polymer [2]. In addition, polymer nanocomposites have excellent barrier properties against gases (e.g., oxygen, nitrogen and carbon dioxide), water and hydrocarbons, strongly dependant on the aspect ratio of clay platelets but not on the chemical interactions and the type of gas or liquid molecules [3]. These improvements with less than 10 wt% addition of single silicate layers with a thickness of about 1 nm and typically lateral dimensions of several hundred nanometers up to micrometers are achieved with good dispersion of clay in the polymer matrix and an optimized interaction at the interface between the two phases [4]. This is in strong contrast to conventional polymer fillers, such as talc, mica, silica, and carbon black that require much higher concentrations (>30 wt%), making processing more difficult and providing only a fraction of these enhancements [5,6].

The most representative layered silicate is natural montmorillonite, i.e. natural smectite clay (2:1 phyllosilicate), which consists of regular stacks of aluminosilicate layers with a high aspect ratio and a high surface area. Because of the hydrated sodium cations in the clay galleries, natural montmorillonite is hydrophilic, which is a problem to have it homogeneously dispersed in organic polymers. Ion exchange of the interlayer inorganic cations by organic cations (i.e. alkylammonium salts or alkyl phosphonium) is an efficient method to provide the clay with organophilicity. Such organo-modified clays are available commercially in several varieties, tailor made for different applications and are compatible with many polymeric materials. Depending on a nanoscale dispersion of the layered silicate, the whole spectrum of structures ranging from intercalated to exfoliated nanocomposites can be observed [7].

The improved properties of nanocomposites are related to the modification of the structure and dynamics of the polymer at and near the particle surface. Because of the large surface area this fraction of the polymer contributes significantly to the properties of the whole nanocomposite, even at low filler content. In this respect polymer nanocomposites are somehow similar to semi-crystalline polymers where the crystals can be considered as nanofillers too [8].

* Corresponding author. Tel.: +389 2 3073 600; fax: +389 2 3065389.
E-mail address: luljeta.raka@unite.edu.mk (L. Raka).

0032-3861/$ – see front matter © 2009 Elsevier Ltd. All rights reserved.
doi:10.1016/j.polymer.2009.05.044

To incorporate nanoparticles in polymer matrices, over the last years several methods have been developed including in situ polymerization, solution blending, and melt mixing [9–11]. Also, interest has grown for the encapsulation of natural clays and the formation of polymer/clay nanocomposites by surfactant-free inverse Pickering emulsion polymerization [12].

Isotactic polypropylene (iPP) is among the most extensively studied thermoplastics with widespread applications, because of its excellent properties and low price. Over the years, iPP has been reinforced with various inorganic or organic fibers (e.g., carbon, glass, Kevlar, PET, PTFE, natural fibers) [13,14] as well as other fillers (talc, mica, calcium carbonate, etc.) [15,16] essentially aiming at improving its mechanical and functional performance [17].

Since iPP is nonpolar polymer, its direct intercalation into the clay galleries is very difficult or impossible to achieve. Overcoming this difficulty, Usuki et al. [18] first reported approach to prepare PP nanocomposites using functional oligomers as compatibilizers, and clays modified with organophilic agents. However, it is well known that functionalization with PP-*g*-MA leads to chain scission of the PP, which usually drastically diminishes the mechanical properties of final composite [19].

Many reports on the different ways of preparations and characterizations of iPP-*g*-MA/clay nanocomposites have been already published [20–24]. Recently a new approach based on latex technology was introduced, which can be successfully applied for preparation of SWCNT/polymer and MWCNT/polymer (CNTs/polymer) conductive composites in a polymer matrix of choice, with very low percolation threshold and potential application in electronics [25–30]. This technique allows a use of third component such as surfactant molecules, to assist the exfoliation of CNTs into the polymer matrix without altering the intrinsic properties of the CNTs. It is a multi-step process for making polymer/CNTs composites which consists of the following steps: (1) an ultrasound-driven exfoliation of the CNTs in water, containing sodium dodecylsulfate (SDS); (2) mixing the stable aqueous CNT dispersions with polymer latex, stabilized by the same surfactant as the CNT dispersion; and (3) freeze-drying, followed by compression molding of the powder into a polymer film [25–27]. The colloidal stability of the CNTs in aqueous SDS solution was quantitatively characterized by UV–vis exhibiting characteristic bands corresponding to additional absorption [29–31]. In addition to being versatile and environmentally friendly, latex technology allows for the achievement of high dispersion qualities, while overcoming the drawbacks of conventional preparation methods. Moreover, it can be easily extended to any matrix polymer synthesized by emulsion polymerization or brought into the form of latex otherwise, such as, PS, PMMA, PE, etc. It favours a great degree of flexibility with respect to the choice of matrix.

The versatility of the 'latex concept' was demonstrated for semi-crystalline polypropylene (PP)/CNT nanocomposites, prepared from aqueous PP emulsions. For this system, a low percolation threshold was found, and the extremely well-dispersed CNTs proved to be excellent nucleating agents for PP, raising significantly the crystallization temperature [17,32]. Nonetheless, to the best of our knowledge, there are no reports of polymer/clay nanocomposites prepared by this new technique. In this paper, we apply the latex technology, previously applied for CNTs/polymer composites, for preparation of iPP/organo-modified clay composites with low loadings of clay particles (1 wt%), with a focus on the crystallization and melting behaviour, thermal and mechanical properties.

Table 1
Nanoclay and its organic modifier[a] (http://www.nanoclay.com).

Grade/supplier	Nanoclay C93A
	Cloisite 93A
	Southern Clay Products, Inc
CEC (meq/100 g clay)	90
Weight loss on ignition (%)	40
Organic modifier	Ternary ammonium salt
Structure of organic modifier	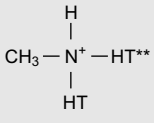
	[b]
Basal spacing, d_{001} (Å)	23.6
Anion	HSO_4^-

[a] Supplier's literature.
[b] HT—Hydrogenated Tallow (~65% C18; ~30% C16; ~5% C14).

2. Experimental section

2.1. Materials

The polymer matrix material is a water-based emulsion of maleic anhydride-grafted isotactic polypropylene (iPP-*g*-MA), commercialized by Solvay S.A. (Belgium, now Addcomp, Netherlands) under the trade name Priex801. It was designed for antistatic applications and contains additives, enhancing its conductivity. According to the supplier, the aqueous emulsion is composed of 25 wt% of iPP polymer and 7 wt% of anionic surfactant of the oleic acid type, neutralized by an amino-alcohol, the remainder being water. The weight-average molar mass of the polymer is in the range $M_w = 50\,000$–$60\,000$ g/mol with about 30 wt% of the iPP below 20 000 g/mol, as determined by GPC in trichlorobenzene using linear polyethylene standards (measured at DSM Resolve, The Netherlands) [17,32]. The surfactant used for the dispersion of clay particles in water was sodium dodecylsulfate (SDS, 90%) provided by Merck Chemical Co. Organically modified clay Cloisite 93A, identified as C93A, was used for the present investigation, and its properties are given in Table 1. All experiments were carried out with demineralized water.

2.2. Preparation of PP/clay nanocomposite

Solutions of 1:2 by weight of bare Cloisite 93A (C93A) and SDS in water were sonicated in a flask with a horn sonicator (Sonics Vibracell VC750) with cylindrical tip (10 mm end cap diameter) at a power of 20 W for 60 min, corresponding to a total energy input of ca. 70 000 J. Since the clay particles are not active in the UV–vis region, its dispersion was observed only visually and left over night to see colloidal stability of the mixtures. The flask was placed in a bath of ice water during sonication in order to prevent rising of the temperature of the mixture. The colloidally stable dispersion of C93A in aqueous SDS was directly mixed with the Priex801 using magnetic stirrer preparing nanocomposites with 1 wt% Cloisite 93A (Scheme 1).

Scheme 1. The schematic representation of the multi-step preparation PP/clay nanocomposites by latex technology.

Then, the obtained mixture was frozen in liquid nitrogen for several minutes and freeze-dried over night using Christ Alpha 2-4 freeze-dryer operated at 0.25 mbar and temperature 20 °C. The resulting degassed composite powder was compressed into films at 180 °C for 30 s at 30 bar and 15 min at 70 bar between poly-(terephthalate) sheets using Collin Press 300G, and then fast cooled to room temperature by press plates containing coils for water. Films of 100–300 μm were produced for WAXD, SEM/TEM, DMTA and DSC experiments.

2.3. Characterization and methods

Wide-angle X-ray diffraction (WAXD) analysis was performed on a Rigaku D/Max-B diffractometer (Japan), equipped with nickel filtered CuKα_1 ($\lambda = 1.54056$ Å) radiation source operated at 40 kV and 25 mA. Corresponding data were collected at step scan rates of 0.02°/min and 1°/min in the range $2\theta = 1.1$–10° for organoclays in powder form and latex samples films.

Transmission electron microscopy (TEM) observation was performed on Tecnai 20 operated in bright-field mode at 200 kV. Ultrathin sections of the PP/clay nanocomposite samples with a thickness of approximately 90 nm were prepared at room temperature using an ultramicrotome Reichert-Jung Ultracut E equipped with a diamond knife. The sections were transferred dry to carbon-coated Cu grids of 200 meshes.

Scanning electron microscopy (SEM) of PP/C93A composite was performed using a Quanta 3D FEG (Fei Co.) equipped with a field-emission gun. High vacuum conditions were applied and a secondary electron detector was used for image acquisition. No additional sample treatment such as surface etching or coating with a conductive layer has been applied before surface scanning.

Thermogravimetric analysis (PerkinElmer TG/DTA Pyris Diamond) was performed in inert atmosphere (under nitrogen) with 2 °C/min heating rate at the temperature range from 20 °C to 500 °C.

Differential scanning calorimetry (DSC) was performed on 5 ± 0.2 mg samples of neat PP and PP/C93A nanocomposite in aluminium pans using a Perkin Elmer DSC 7 analyzer. Calibration of the instrument was done using standards samples of In and Zn. Each sample was heated from −45 °C to 240 °C (first run), hold at 240 °C for 5 min to erase the previous thermal history, cooled down to −45 °C at 10 °C/min cooling rate (second run). After cooling, a heating run to 240 °C was performed at 10 °C/min. All runs were carried out in a stream of nitrogen.

Dynamic mechanical thermal analysis (DMTA) of PP latex and PP/clay nanocomposites was performed on a TA Instruments DMAQ800 machine fitted with a tensile testing head. A rectangular strip was cut from the compression-molded film. The system was automatically cooled to −50 °C, and then heated at a rate of 3 °C/min to 150 °C under nitrogen flow. The samples were scanned at fixed frequency of 1 Hz and amplitude of 10 μm was used. A static force of 10 mN was applied to ensure that the sample was taut between the tensile grips. The force was kept constant during the test to allow shrinkage of the sample during testing.

3. Results and discussion

3.1. Morphological analysis

WAXD technique is usually used to study the formation of nanocomposite structure (intercalated or exfoliated) by monitoring the 2θ position of the clay diffraction peaks (d_{001} and d_{002}) in PP matrix using Bragg's law, and shape and intensity of basal reflections from the distributed silicate layers.

Fig. 1 shows the WAXD patterns of the organically modified clay (Cloisite 93A), neat PP and PP/C93A nanocomposite containing

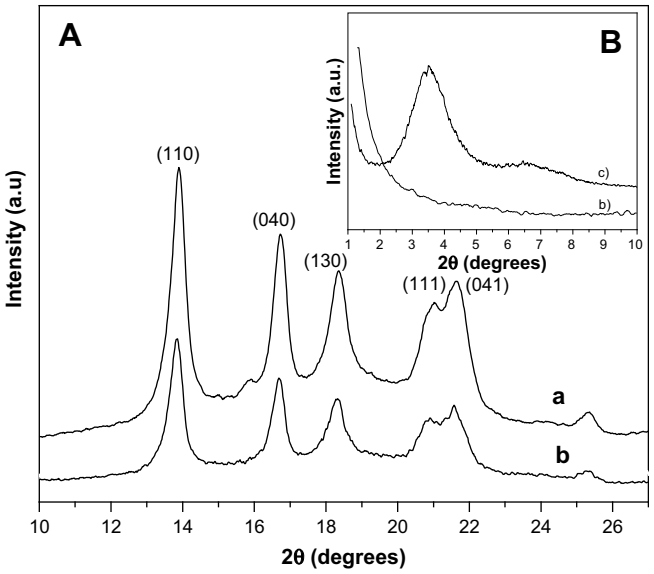

Fig. 1. WAXD patterns for: A—neat PP (a) and nanocomposite containing 1 wt% C93A (b) in $2\theta = 10°$–26°, B—nanocomposite (b) and Cloisite 93A (c) in $2\theta = 1.0°$–10°, showing the absence of clay characteristic peak at $2\theta \sim 3.5°$.

1 wt% C93A. For the Cloisite 93A, a peak appeared at $2\theta \sim 3.5°$, corresponding to the basal spacing of silicate galleries (d_{001}) of 2.51 nm (Fig. 1c). A second broad peak was observed in a clay pattern at $2\theta \sim 6.6°$ due to the presence of nonmodified portion of natural clay, corresponding to the basal spacing of silicate galleries (d_{002}) of 1.34 nm. The absence of main clay peaks in the investigated nanocomposite sample containing 1% C93A (Fig. 1b) could be a sign that possible clay exfoliation in the PP matrix has occurred. This, in turn, may be a result of strong interaction between polar groups of PP-*g*-MA molecule and the silicate layer. However, the results provided only by WAXD technique cannot be used for nanocomposite data interpretation because they cannot determine the internal structure and spatial distribution of the silicate layers as well as any structural non-homogeneity in the observed nanocomposite, although the disappearance of diffraction peak in WAXD scans in Fig. 1 is observed.

In order to visualize the dispersion of nanoclay particles C93A into the PP matrix and to support the interpretation of WAXD patterns, TEM investigations have been performed. Fig. 2 shows the bright-field TEM micrographs of clay particles C93A in the PP matrix at clay loading of 1 wt% at low and high magnifications. The dark areas in TEM images represent the clay particles and the grey ones the continuous PP matrix. As can be seen from Fig. 2, while WAXD data indicate complete exfoliation of clay in the matrix (absence of clay characteristic peak) (Fig. 1b), exfoliated single clay and some stacks of clay layers can be found in TEM image. According to the observation from TEM and WAXD analysis intercalated/exfoliated nanocomposites are indicated. The interface between clay particles and the surrounding PP matrix is enlarged due to diffusion of the polymer into clay galleries, leading to more extensive exfoliation of clay particles. According to some authors [1] the observed peculiarities in the structure originate from the strong hydrogen bonding between the maleic anhydride groups of the matrix and the polar clay surface.

Many reports of iPP-*g*-MA/clay nanocomposites have been published already showing the effect of addition of clay to the polymer matrix on the clay layers spacing (intercalation/exfoliation) and the effect the clay intercalation/exfoliation on the crystallization and melting behavior, and mechanical properties of the polymer matrix [20–24]. Using XRD and TEM analysis some studies found that there

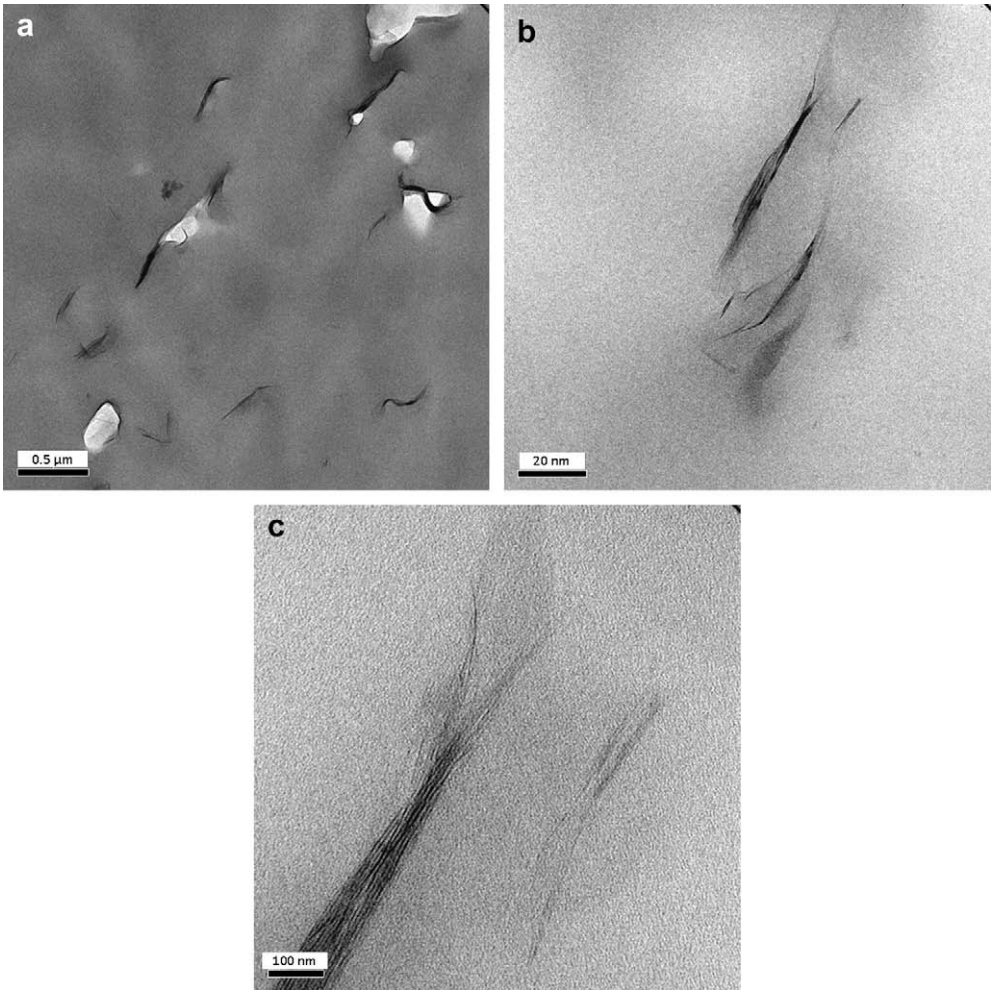

Fig. 2. Bright-field TEM micrographs of PP nanocomposite containing 1 wt% C93A at different magnification. Exfoliated single clay layers (c) and some stacks of clay layers (b, c) are clearly seen.

was some intercalation and partial exfoliation in the clay particles which was accompanied by improvement in mechanical properties [33,34], others proved complete exfoliation [35].

Another study reported for significant exfoliation of the clay was based on an increase in mechanical properties, absence of clay peaks in XRD analysis and SEM images [36]. The confidence on XRD data and the lack of TEM images to support these observations can lead to incorrect conclusions being drawn regarding the state of exfoliation in a polymer/clay composite.

Fig. 3 shows SEM images of the surface of a PP/C93A nanocomposite with a C93A concentration of 1 wt%. The clay nanoparticles appeared to be coated by PP phase. Some voids caused by incorporation of nanoscale clay particles in a matrix are also seen, probably arisen as a result of shrinkage during crystallization; it

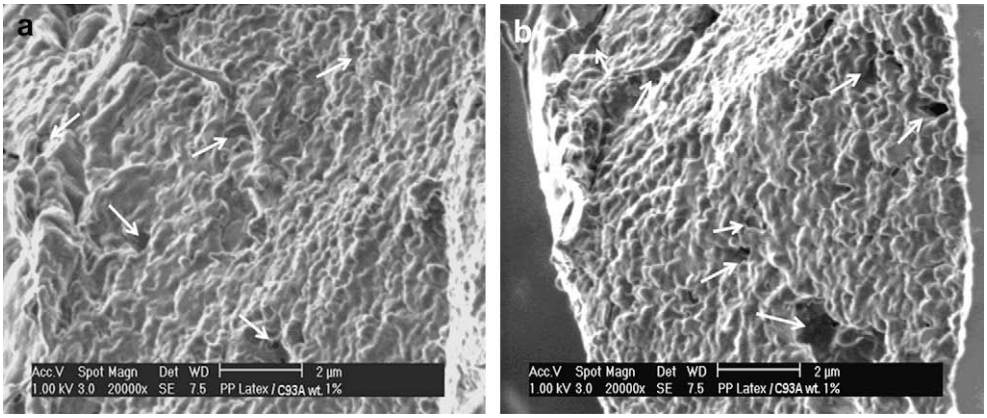

Fig. 3. SEM micrographs of PP nanocomposite sample with 1 wt% C93A (white arrows indicates the presence of voids).

represents an additional indication on good polymer/clay interfacial adhesion.

3.2. Thermal behavior of the nanocomposites

In this study, the thermal properties of PP/organo-modified clay nanocomposites are investigated, aiming at assessing the changes in the thermal behavior of the PP matrix, induced by the presence of low loading of organo-modified clay.

The percent weight loss versus temperature of the organo-modified clay C93A, neat PP and PP nanocomposite, obtained by TGA in inert atmosphere is presented in Fig. 4.

Obviously, the thermal stability of the matrix is affected by the presence of clay particles. The increased thermal stability of the nanocomposite might be attributed to the enhanced interface interactions, as discussed earlier. Our previous TGA/DTG investigations have shown an improved thermal stability of PP/organoclay nanocomposites (containing 1–3% nanoclay) in oxygen atmosphere as well. Significant prolongation of oxidation induction time (measured at 200 °C) for nanocomposite containing 1% organo-modified clay has been also found [37].

Extensive research has been shown that the addition of fillers/fibers (carbon, glass, PET, etc) [13,14] and different nanofillers (CNTs/fibers or layered silicates) significantly affects crystallization behaviour and resulting crystalline morphology of the iPP matrix, and also strongly modifies the kinetics of the crystallization process as a result of their nucleating action [14,17,38]. The crystalline structure is expected to significantly influence physical and mechanical properties of polymer nanocomposites. Nonisothermal crystallization kinetics of polymer nanocomposites has been studied extensively for different polymer/filler systems, including PP/clay [20,38,39], PP/carbon nanotubes [16], PP/SiO_2 [40]. In general, there are two effects of clay silicate layers on the crystallization behavior of polymer matrix which are related to the content and dispersion of clay: (i) heterogeneous nucleation accompanied by decrease of the interfacial free-energy per unit area and (ii) restriction of the polymer chain motion causing decrease of a crystallinity and degree of perfection of the crystals [41]. The elevation of nonisothermal crystallization peak temperature due to the presence of clay/filler was found in composites prepared by melt blending of organo-modified clay with iPP [38].

In order to quantify the effects of clay layers on the crystallization behaviour of the PP matrix, nonisothermal crystallization experiments from the melt at a cooling rate of 10 °C/min were carried out. As shown in Fig. 5, the addition of even low loadings (1 wt% C93A) into the PP matrix, when cooled from melt, leads the crystallization of PP filled with C93A to start at higher temperatures as compared to that of the neat PP. The crystallization onset temperature (T_c,onset) rises about 5 °C (from 110 °C for the neat iPP to 115 °C for PP/clay composites). This finding demonstrates the possible nucleating effect of clay particle in a PP matrix providing sites for heterogeneous nucleation and contributing to the creation of different morphological features during the heterogeneous nucleation process [42]. Similar nucleation effects were also reported for other polymer/clay nanocomposites [38,43,44]. The extent of increase in crystallization temperature varied slightly with the type of clay/filler (about 5 °C increase with addition of 3–5 wt% organo-modified clay) [45] and type of compatibilizing agents used [21,46]. Perrin-Sarazin et al. [47] noted that the kinetics of crystallization is not only related to the clay content, but also depends on PP–clay interactions. In absence of the coupling agent the crystallization of PP occurred at higher temperature and at a higher rate than neat PP, but the crystallization behaviour was similar to neat PP when coupling agent was added. Svoboda et al. [48] have found that the increase of rate of isothermal crystallization proceeds only in PP/PP-*g*-MA/clay systems containing clay tactoids, while no clay nucleation ability in systems with well dispersed clay was observed. Qian et al. [49] noted that addition of 1 wt% SiO_2 nanoparticles in the PP matrix increases the onset crystallization temperature for about 4 °C. Lu et al. [17] have shown that SWCNTs and MWCNTs for low loadings strongly nucleate the iPP, when cooling the sample from the quiescent melt, rising the onset crystallization temperature for about 9 °C and 14 °C, respectively.

The crystallinity of PP/clay nanocomposites, calculated from the enthalpy of melting (ΔH_m = 80 J/g) compared to neat PP (ΔH_m = 82.2 J/g), is slightly decreased probably due to different achieved degree of perfection of the crystals as a result of physical hindrance of clay layer to the motion of polymer chain by the presence of clay layers in a PP matrix [50]. The overall crystallization process is accelerated as a result of the presence of clay particles, providing a tremendous amount of sites for heterogeneous nucleation and increasing the onset temperature of crystallization with respect to the homogeneously nucleated neat PP. It should be mentioned that for iPP/CNTs composites changes in the developed degree of crystallinity based on a comparison between the recorded enthalpies for all samples could not be observed [17].

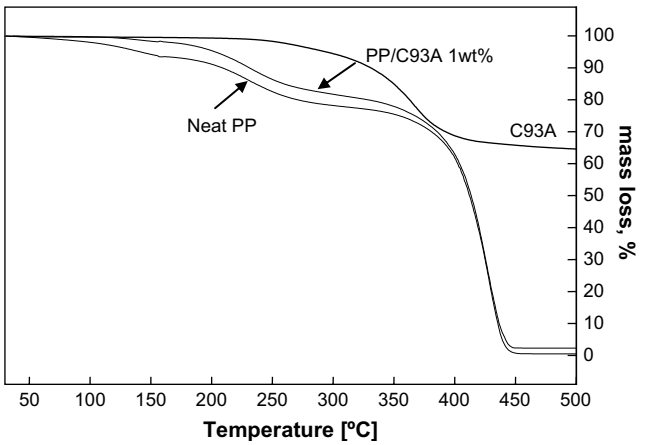

Fig. 4. TG curves in inert atmosphere for: C93A, neat PP and PP/C93A containing 1 wt% (heating rate 2 °C/min).

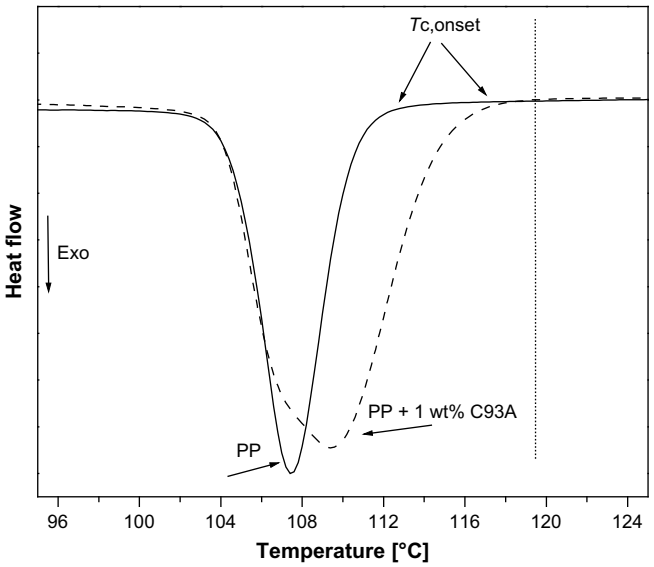

Fig. 5. DSC cooling scans (cooling rate 10 °C/min) of neat PP and nanocomposite containing 1 wt% C93A (crystallization from quiescent melt).

From the obtained crystallization curves the following parameters are determined: (1) the initial slope of the exotherm at inflection on the high-temperature side, S_i, and (2) the width at half height of the exothermic peak, ΔW [51]. The S_i indicates relative kinetics of the nonisothermal crystallization process, and higher absolute values of S_i suggest faster crystallization. The crystallization of neat PP sample is faster ($S_i = 5.67$ a.u.) than of nanocomposite one ($S_i = 3.27$ a.u.), although the crystallization of the latter starts at higher temperature compared to neat PP. ΔW refers to the distribution of the forming crystal dimensions; i.e. the smaller the ΔW, the narrower the distribution. It can be seen that the distribution of the crystal dimensions in nanocomposite is broader than in neat PP for about 48%. Some authors reported that the addition of organo-clays into crystalline matrix do not ensure the enhancement of the polymer matrix crystallization rate. Different crystal forms formation and/or the specific interaction between organo-clays and polymer matrix might cause the reduction of polymer chain mobility upon crystallization [52]. The rate-determining factor could be a limitation in the diffusion of polymer chains toward the growing front, which might result from reduced polymer mobility and from the chain diffusion in a geometrically confined space [17].

The melting behaviour was investigated after nonisothermal crystallization at a heating rate of 10 °C/min, and the melting traces of neat PP and nanocomposite sample are shown in Fig. 6. As can be seen, multiple melting peaks were observed in both samples. The presence of organo-modified clay has no excessive influence on the melting behavior of the matrix material. Whereas the neat PP clearly shows double melting behavior, the shape of the melting transition changed toward multiple broader melting peaks with addition of low clay loadings. Indeed, the high melting peak $T_{m,2}$ of nanocomposite slightly shifts to lower values, whereas the lower melting peak $T_{m,1}$ is consisted of two overlapped peaks.

The appearance of multiple melting behaviours is generally assumed to result from existence of different crystal structure (polymorph), from successive melting of crystals with distinct degrees of perfection, or from the rapid succession of melting–crystallization–melting or recrystallization phenomena [17]. Petracone et al. reported that the double melting peaks may be attributed to the existence of less-ordered α_1 and more-ordered α_2 forms with a well-defined deposition of up and down helices in the unit cells [53]. The impact of filler/clay on the polymorphic behaviour of PP has been extensively investigated over the years [54]. Some authors reported that clay nanoparticles can induce crystallization of iPP in the monoclinic α- and γ-form but significantly inhibit formation of β-phase crystallites [55]. Grady et al. [56] showed that both melting–recrystallization–melting and polymorphism induce appearance of multiple melting peaks in PP/SWNT composites, without providing evidence from WAXD experiments.

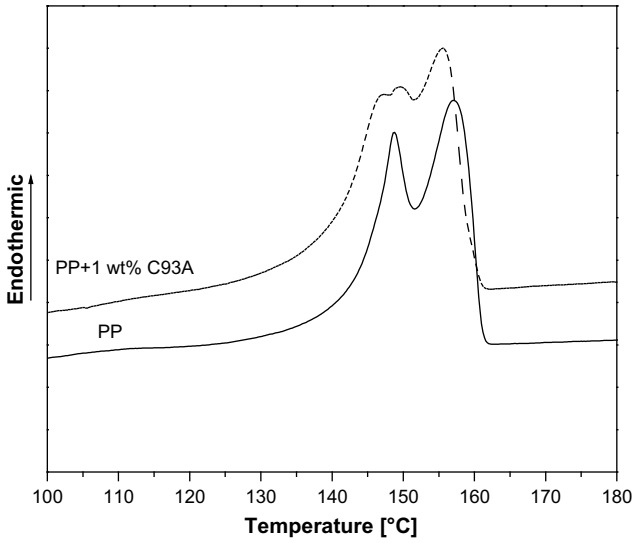

Fig. 6. DSC melting thermograms recorded during heating rate at 10 °C/min of neat PP and nanocomposite containing 1 wt% after crystallization from quiescent melt (cooling rate 10 °C/min). The appearance of multiple melting peaks in PP/CNTs nanocomposites has been discussed in detail in our previous paper [17].

As can be seen from Fig. 1, the typical pattern of α-crystalline PP is found, with no indication of β-phase PP. It can therefore be concluded that organo-modified clay have a strong α-nucleating effect on PP and that the complex melting transition of the nanocomposites originates from the fusion of polymer crystals with varying lamellar thicknesses, either simultaneously present or as a result of recrystallization phenomena [17].

The double-melting peaks also appeared when the samples of PP/C93A nanocomposites were isothermally crystallized at low T_c (115 °C), which disappears as T_c increases. The same behavior has been observed in iPP/fiber model composites [23,24]. From corresponding thermal analysis studies carried out on PP/CNTs composites using the latex-based route for the preparation of nanocomposites, as introduced above, any influence of grafted maleic anhydride and the surfactant used for stabilization of the CNT and iPP latex dispersion on the crystallization behaviour and the crystal orientation on the iPP can be excluded. Surfactant molecules are exchanged with low molar mass polymer chains of the matrix material during thermal treatment [17].

3.3. Dynamic mechanical analysis

The properties of nanocomposites are strongly influenced by the nature of filler/matrix interface, and as it was shown the latex technology offers an improved interfacial behaviour [17,32]. Samples of neat iPP and PP/clay nanocomposites containing 1 wt% C93A were subjected to dynamic mechanical tests to study viscoelastic characteristics and relaxation processes. The dynamic storage modulus (E') and loss tan δ factor as a function of temperature are recorded in the temperature range from −50 °C to 150 °C and the results are presented in Fig. 7.

From Fig. 7a it is evident that incorporation of nanoclay resulted in an increase in the storage modulus of PP matrix compared to neat PP, which is ascribed to the exfoliation of the organo-clay platelets in PP matrix at nanoscale level and the restricted segmental motion at organic/inorganic interface. This indicates the possible reinforcing effect of layered silicate and improvement of the thermal–mechanical stability of PP/clay nanocomposites [45]. The storage modulus for all investigated samples converges to a close value after approaching the melting temperature ($T_m = 155$–157 °C) because of the softening effect. The results of DMTA are summarized in Table 2.

The addition of 1 wt% C93A in PP matrix particularly at temperature higher than T_g caused the storage modulus to increase by approximately 30%. With increasing the temperature, this difference becomes smaller. Similar increase in the dynamic storage modulus is reported for other polymer/filler nanocomposites [43,56]. Hambir et al. [46] found that the extent of increase in the storage modulus is dependent on the type of compatibilizer used (about 20%–50%) attributed to the presence of clay particles in the PP matrix. Grady et al. [56] found very little difference in the small strain mechanical properties between filled and unfilled polymers of about 15% with addition of 1.8 wt% carbon nanotubes and no gain in storage modulus was found for sample filled with 0.6% nanotubes without measurable change in the glass transition

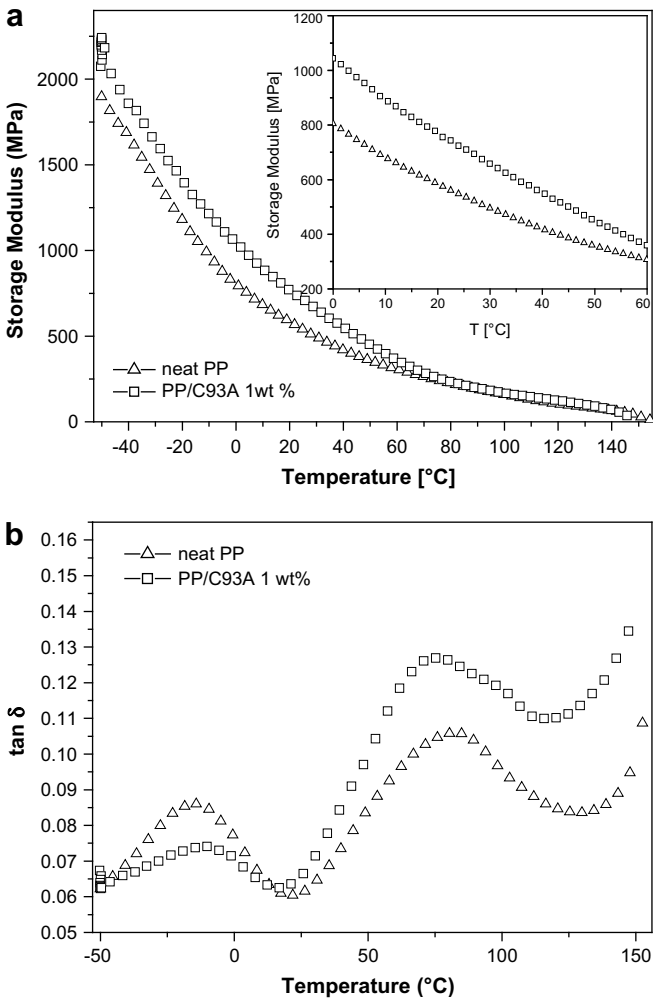

Fig. 7. Temperature dependence of dynamic storage modulus E' (a) and tan δ (b) for neat PP matrix and PP/C93A 1 wt% nanocomposites.

temperature. Lozano and Barrera [57] showed that the addition of 2 wt% carbon fibres caused the storage modulus at room temperature to increase by approximately 60%. The tan δ curves represent the ratio of dissipated energy to the stored energy and are related to the glass transition temperature of the polymer. McCrum et al. [58] have demonstrated that the tan δ curve of PP exhibits three relaxation localized in the vicinity of −80 °C (γ), 10 °C (T_g) and 100 °C (α). The second high-temperature wide peak in tan δ–T curve is observed frequently for semi-crystalline polymers and is associated with the phenomena such as intracrystalline relaxation (α-relaxation) and sliding of tied chains within crystalline blocks of PP.

From the dependence loss tan δ versus temperature (Fig. 7b) two major transitions can be evidenced for each sample: one at −15 °C and another broad peak between 60 °C and 90 °C. The first maximum corresponds to the glass transition region and the second, broader, transition around 80 °C is attributed to T_g of the rigid amorphous phase of iPP [59]. The tan δ peak value is found to be slightly lower for the nanocomposite containing 1 wt% C93A compared to neat PP, suggesting restricted cooperative motion of polymer chains at that temperature. Also, the crystalline fraction in PP/clay nanocomposites calculated from the heat of melting is comparable to that of neat PP, and therefore this decrease in a value of tan δ could be ascribed to the presence of the constrained fraction in PP/clay nanocomposites [45].

Table 2
Dynamic storage moduli of neat PP and nanocomposite at various temperatures and glass transition temperatures, T_g values obtained from tan δ.

Sample	Storage modulus (MPa)				T_g (°C)	tan δ_{max}
	−50 °C	0 °C	50 °C	100 °C		
Neat PP	1896	804.7	356.4	157	−16.38	0.090
PP/C93A1 wt%	2094	1044	450	168	−14.63	0.074

The key factors for producing such composites with low clay loadings comprise the quality of the wetting between the filler and the polymer matrix, as well as the state of dispersion of the clay particles throughout the matrix [60].

4. Conclusions

In the present study, we have demonstrated successful application of latex technology for preparation of PP/organo-modified clay nanocomposites, which has been previously used for preparation of CNTs/polymer composites. After ultrasonication-driven exfoliation of clay nanoparticles, mixing with PP latex, freeze-drying and subsequent compression molding, dispersion of organo-clay particles at nanoscale level in the matrix polymer was observed confirmed by morphological analysis carried out by WAXD and TEM/SEM. According to the results of WAXS and TEM analysis, even WAXD data showed complete exfoliation of clay in the matrix (absence of clay characteristic peak); in TEM image some stacks of clay layers can be found. An increased thermal stability of nanocomposite sample compared to neat PP in inert atmosphere was revealed by TGA. Calorimetric investigations have shown that clay particles act as nucleation agents for iPP, which increases its crystallization temperature when cooling from the quiescent melt. The complex multiple melting behavior was interpreted in terms of recrystallization phenomena occurring during heating. The storage modulus of the nanocomposites increased for 30%, particularly at temperature higher than T_g, confirming the reinforcing effect of clay in PP matrix.

Acknowledgments

The present study was supported by COST Action P12 "Structuring of Polymers", COST-STSM-P12-02842. Thanks are due to The Ministry of Education and Science of Republic of Macedonia for the financial support of the COST-related project activities. In addition, we would like to thank Marco Hendrix from the Department of Chemical Engineering and Chemistry, Eindhoven University of Technology for WAXD measurements.

References

[1] Ray SS, Okamoto M. Prog Polym Sci 2003;28(11):1539–641.
[2] Gilman JW. Appl Clay Sci 1999;15:31–49.
[3] Zeng QH, Yu AB, (Max) Lu GQ, Paul DR. J Nanosci Nanotechnol 2005;5:1574–92.
[4] Rzaev ZMO, Yilmazbayhan A, Alper E. Adv Polym Technol 2007;26(1):41–55.
[5] Kawasumi M, Hasegawa N, Kato M, Usuki A, Okada A. Macromolecules 1997;30:6333–8.
[6] Lebaron PC, Wang Z, Pinnavaia T. Appl Clay Sci 1999;15:11–29.
[7] Lepoittevin B, Pantoustier N, Devalckenaere M, Alexandre M, Calberg C, Jérôme R, et al. Polymer 2003;44(7):2033–40.
[8] Sargsyan A, Tonoyan A, Davtyan S, Schick C. Eur Polym J 2007;43:3113–27.
[9] Gilman JW, Morgan AB, Harris RH, Trulove PC, Delong HC, Sutto TE. Polym Mater Sci Eng 2000;83:59–60.
[10] Vaia RA, Vasudevin S, Krawiec W, Scanlon LG, Giannelis EP. Adv Mater 1995;7:154–6.
[11] Giannelis EP. Adv Mater 1996;8:29–35.
[12] Voorn DJ, Ming W, Van Herk AM. Macromolecules 2006;39:2137–43.
[13] Lee GW, Jagannathan S, Chae HG, Minus ML, Kumar S. Polymer 2008;49(7):1831–40.
[14] Bogoeva-Gaceva G, Grozdanov A. J Serb Chem Soc 2006;71(1):483–99.
[15] Moniruzzaman M, Winey KI. Macromolecules 2006;39(16):5194–205.
[16] Bhattacharyya AR, Sreekumar TV, Liu T, Kumar S, Ericson LM, Hauge RH, et al. Polymer 2003;44:2373–7.

[17] Miltner HE, Grossiord N, Lu K, Loos J, Koning CE, Van Mele B. Macromolecules 2008;41:5753–62.
[18] Usuki A, Kato M, Okada A, Kurauchi T. J Appl Polym Sci 1997;63:137–9.
[19] Manias E, Touny A, Wu L, Chung TC, Gilman JW. Polym Mater Sci Eng 2000;82:282–3.
[20] Wu JY, Wu TM, Chen WY, Tsai ShJ, Kuo WF, Chang GY. J Polym Sci B Polym Phys 2005;43:3242–54.
[21] López-Quintanilla ML, Sánchez-Valdés S, Ramos de Valle LF, Guedea Miranda R. Polym Bull 2006;57:385–93.
[22] Zhang YQ, Lee JH, Jang HJ, Nah ChW. Compos B Eng 2004;35(2):133–8.
[23] Guduri BR, Luyt AS. J Nanosci Nanotechnol 2008;8:1880–5.
[24] Nejad SJ, Ahmadi SJ, Hossein A, Mohaddespour A. J Appl Sci 2005;7(17):2480–4.
[25] Regev O, ElKati PNB, Loos J, Koning CE. Adv Mater 2004;16(3):248–51.
[26] Grossiord N, Loos J, Koning CE. J Mater Chem 2005;15:2349–52.
[27] Loos J, Alexeev A, Grossiord N, Koning CK, Regev O. Ultramicroscopy 2005; 104:160–7.
[28] Yu J, Lu K, Sourty ED, Grossiord N, Koning CE, Loos J. Carbon 2007;45(15): 2897–903.
[29] Grossiord N, Regev O, Loos J, Meuldijk J, Koning CE. Anal Chem 2005;77:5135–9.
[30] Yu J, Grossiord N, Koning CE, Loos J. Carbon 2007;45(3):618–23.
[31] Grossiord N, Loos J, Meuldijk J, Regev O, Miltner E, Van Mele B, et al. Compos Sci Technol 2007;67(5):778–82.
[32] Lu K, Grossiord N, Koning CE, Miltner HE, Van Mele B, Loos J. Macromolecules 2008;41(21):8081–5.
[33] Ding C, Jia D, He H, Guo B, Hong H. Polym Test 2005;24:94–100.
[34] Zhang Q, Fu O, Jiang L, Lei Y. Polym Int 2000;49:1561–4.
[35] Zhang Y, Lee J, Rhee J, Rhee K. Compos Sci Technol 2004;64:1383–9.
[36] Tzavalas S, Macchiarola K, Gregoriou VG. J Polym Sci B Polym Phys 2006;44:914–24.
[37] Bogoeva-Gaceva G, Raka L, Dimzoski B. Adv Compos Lett 2008;17(5):161–4.
[38] Xu W, Liang G, Zhai H, Sh Tang, Hang G, Pan WP. Eur Polym J 2003; 39:1467–74.
[39] Yuan Q, Awate S, Misra RDK. Eur Polym J 2006;42:1994–2003.
[40] Papageorgiou GZ, Achilias DS, Bikiaris DN, Karayannidis GP. Thermochim Acta 2005;427:117–28.
[41] Novacki R, Monasse B, Piorkowska E, Galeski A, Haudin JM. Polymer 2004; 45:4877–92.
[42] Liu ZJ, Chen KQ, Yan DY. Eur Polym J 2003;39:2359–66.
[43] Hu W, Ge M, He P. J Polym Sci B Polym Phys 2002;40(5):408–14.
[44] Maiti P, Nam PH, Okamato M, Hasegawa N, Usuki A. Macromolecules 2002;35(6):2042–9.
[45] Samal SK, Nayak SK, Mohanty S. J Thermoplast Compos Mater 2008;21:243–63.
[46] Hambir S, Bulakh N, Jog JP. Polym Eng Sci 2002;42:1800–7.
[47] Perrin-Sarazin F, Ton-That MT, Bureau MN, Denault J. Polymer 2005;46: 11624–34.
[48] Svoboda P, Zeng C, Wang H, Lee LJ, Tomasko DL. J Appl Polym Sci 2002;85(7):1562–70.
[49] Qian J, He P, Nie K. J Appl Polym Sci 2004;91:1013–9.
[50] Wang K, Xiao Y, Na B, Tan H, Zhang Q, Fu Q. Polymer 2005;46:9022–32.
[51] Wang JL, Dong CM. Polymer 2006;47:3218–28.
[52] FCh Chiu, Chu PH. J Polym Res 2006;13:73–8.
[53] Petracone V, Guerra G, De Rossa C, Tuzi A. Macromol Chem Rapid Commun 1984;5:631–4.
[54] Varga JJ. J Macromol Sci 2002;4:1121–71.
[55] Zheng W, Li X, Ton CL, Zheng TH, He C. J Polym Sci B Polym Phys 2004;42:1810–6.
[56] Grady BP, Pompeo F, Shambaugh RL, Resasco DE. J Phys Chem B 2002;1006:5852–8.
[57] Lozano K, Barrera E. J Appl Polym Sci 2001;79:125–33.
[58] McCrum NG, Read BE, Williams G. Anelastic and dielectric effects in polymeric solids. London: Wiley; 1967.
[59] Wunderlich B. Progr Polym Sci 2003;28:383–450.
[60] Grossiord N, PhD thesis, 2007, available from the website of the Eindhoven University Library (http://www.tue.nl/nl/diensten/bib).